Z. Phys. A 351, 199–208 (1995)

ZEITSCHRIFT
FÜR PHYSIK A

Importance of gluon-gluon and quark-antiquark contributions to charmonium production in proton-proton and antiproton-proton collisions

P.-B. Gossiaux[1], **J. Cugnon**[2]

[1]Laboratoire de Physique Nucléaire, Université de Nantes, Rue de la Houssinière, 57, F-44072 Nantes Cedex 03, France
[2]Institut de Physique B5, Sart Tilman, Université de Liège, B-4000 Liège 1, Belgium

Received: 24 June 1994/Revised version: 13 September 1994

Abstract. The importance of the gluon-gluon and quark-antiquark contributions to the production of charmonium states in proton-proton and antiproton-proton collisions is determined within the parton model in a way which does not rely on any assumption on the dynamics (leading diagrams, color neutralisation mechanism, ...). It is shown that the combined analysis of total and differential inclusive J/ψ production cross-sections for both systems allows such a determination. The primordial contributions are also extracted at one energy. The implications of the numerical values are also discussed.

PACS: 13.85.Ni; 13.85.-t

I. Introduction

The production of charmonium and bottomium states in hadron-hadron collisions is supposed to be dominated by parton-parton interactions. If the two partons are in a colourless state, the direct production of (solely) a $J^{PC} = 1^{--}$ state (J/ψ and ψ') in the s-channel is forbidden by angular momentum, parity and charge conjugation conservation [1–4]. However, such a state can be produced indirectly, by decay of $J^{PC} = 1^{++}$, 2^{++} states (the χ's e.g.) which can be formed directly within the colour singlet model. On the other hand, if the two partons are in a colour (octet) state, a "coloured" 1^{--} object can be produced directly, and a colourless 1^{--} meson can be formed only if some colour neutralisation mechanism has taken place. Such a possibility is embodied for instance the so-called colour evaporation model [5, 6]. If one disregards mechanisms involving the interaction of three (or more) initial partons (and the possible presence of intrinsic heavy flavour in ordinary hadrons), the production of 1^{--} mesons necessarily proceeds either through gluon-gluon interaction or quark-antiquark interaction.

The relative importance of the respective mechanisms is not really well known. The usual method for tentatively determining it relies on model calculations for evaluating one of these mechanisms. This procedure is however not very reliable, as calculations are usually performed to lowest order and, furthermore, as often only one part of the process is included in the calculation. This paper is an attempt to overcome these limitations and to determine the importance of gluon-gluon and of quark-antiquark contributions without relying on model calculations, just by the analysis of the experimental data. Of course, this cannot be done without a minimum number of reasonable hypotheses, which are explained below. Our strategy is to see whether present experimental data can be explained within these hypotheses, only allowing an adjustable importance of the two above mentioned contributions.

II. Procedure

As we said in the Introduction, we assume that the interactions of three (or more) initial partons are unimportant, as well as the contribution of intrinsic charm (here we limit ourselves to charm production). We furthermore assume, as usual, that the charmed quarks contained in a 1^{--} meson are formed on-shell or, in other words, that meson internal wavefunction effects are unimportant. Finally, we assume the validity of the parton model. We are thus considering processes which correspond to the generic diagram drawn in Fig. 1 (where i and j denote the two initial partons). In this diagram, the bubble represents anything which can lead to colour neutral mesons, whatever the colour in the initial two partons state, and which, within the parton model can be described by effective cross-sections. It should be understood that, if the initial two parton state is coloured, an unidentified outgoing object, carrying out the colour, should be attached to the bubble of Fig. 1. We assume that the colour neutralisation mechanism does not affect sensitively the energy-momentum flow. In other words, whatever the mechanism for eliminating the colour possibly carried by the $c - \bar{c}$ pair

* Supported by contract SPPS-IT/SC/29

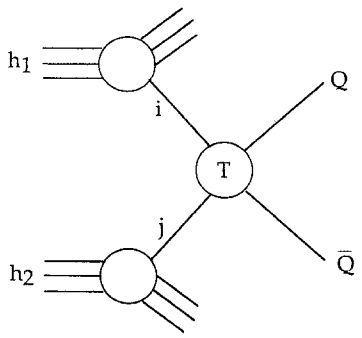

Fig. 1. Generic diagram for heavy flavour production in hadron-hadron collisions

directly formed, we assume that the energy-momentum of the final c-$\bar{c}$ pair is not really modified, or that energy-momentum conservation applies through the bubble (for the four indicated legs of the bubble). Of course, the diagram of Fig. 1 describes only the primordial production, and the usual decay scheme (e.g. $\chi \to J/\psi + \gamma$) should be accounted for.

Some of the assumptions above may be questioned. We are aware of this and comment on it in Sect. VI. Our philosophy is to consider these assumptions as our starting point and to see whether the data can be described within this scheme. We will see below that we can answer positively to this question.

III. Basic formulae

The total cross-section for the formation of a primordial meson of mass M_1, can be given, with the assumption of Sect. II and adopting the usual notation of the parton model, as [1]

$$\sigma_{\text{prim}}(M_1) = \sum_{\{i,j\}} \sigma_{\text{eff}}^{ij}(M_1) \int_{\tau_1}^{1} \frac{\mathrm{d}x}{x} f_i(x) f_j\left(\frac{\tau_1}{x}\right) \mathrm{d}x, \tag{III.1}$$

where $\{i,j\}$ is either $\{g,g\}$, $\{\bar{q},q\}$, or $\{q,\bar{q}\}$ taking into account the fact that the quark can come either from the incident hadron or from the target. As usual, f_i and f_j are the structure functions of the projectile and target hadrons and $\tau_1 = (M_1^2/s)$, $\sqrt{s}$ being the total c.m. energy. The quantities $\sigma_{\text{eff}}^{i,j}$ are the effective cross-sections corresponding to the two basic mechanisms. With the assumptions above, they can be considered as functions of M_1 only. They are the quantities that we want to determine from the data. Equation (III.1) can be rewritten as

$$\sigma_{\text{prim}}(M_1) = \sum_{\{i,j\}} \sigma_{\text{eff}}^{ij}(M_1)\, I_{ij}(\tau_1). \tag{III.2}$$

This formula has the appealing property that the dynamics is contained in the quantities $\sigma_{\text{eff}}^{ij}(M_1)$ whereas the kinematics is contained in the phase space integrals $I_{ij}(\tau_1)$. In case of possible confusion, we will use the detailed notation $I_{ij}^{h_1 h_2}$ in order to specify the projectile h_1 and target h_2 hadrons.

The production cross-section of a meson M_0 after decay of primordial mesons may be written in all generality as

$$\sigma^{\text{tot}}(M_0) = \sum_{M_1} \sigma_{\text{prim}}(M_1)\, BR\,(M_1 \to M_0) + \sigma_{\text{prim}}(M_0)\left(1 - \sum_{M_1'} BR(M_0 \to M_1')\right), \tag{III.3}$$

where $BR(M_k \to M_l)$ is the branching ratio for the decay of meson M_k into Meson M_l. One may rewrite (III.3), using (III.2), as

$$\sigma^{\text{tot}}(M_0) = \sum_{\{i,j\}} \sigma_{\text{eff}}^{ij,\text{tot}}(M_0) I_{ij}(\tau_0), \tag{III.4}$$

with

$$\sigma_{\text{eff}}^{ij,\text{tot}}(M_0) = \sum_{M_1} \sigma_{\text{eff}}^{ij}(M_1) BR(M_1 \to M_0) \frac{I_{ij}(\tau_1)}{I_{ij}(\tau_0)} + \sigma_{\text{eff}}^{ij}(M_0)\left(1 - \sum_{M_1'} BR(M_0 \to M_1')\right), \tag{III.5}$$

or simply

$$\sigma_{\text{eff}}^{ij,\text{tot}} \approx \sum_{M_1} \sigma_{\text{eff}}^{ij}(M_1) BR(M_1 \to M_0) + \sum_{M_1'} \sigma_{\text{eff}}^{ij}(M_0)\left(1 - \sum_{M_1'} BR(M_0 \to M_1')\right), \tag{III.6}$$

if one disregards the thiny difference between $I_{ij}(\tau_0)$ and $I_{ij}(\tau_1)$ for the range of masses and the range of values of s that we will consider below.

The differential cross-sections assuming isotropic decay of primordial mesons, are given by:

$$\frac{\mathrm{d}\sigma^{\text{tot}}(M_0)}{\mathrm{d}x_F} = \sum_{M_1, M_2} \int_{x_F', \text{low}}^{x_F', \text{up}} \frac{\mathrm{d}\sigma_{\text{prim}}(M_1)}{\mathrm{d}x_F'} \frac{\mathrm{d}N}{\mathrm{d}x_F}(x_F') \times \mathrm{d}x_F' BR(M_1 \to M_0 + M_2) + \frac{\mathrm{d}\sigma_{\text{prim}}(M_0)}{\mathrm{d}x_F}\left(1 - \sum_{M_1'} BR(M_0 \to M_1')\right), \tag{III.7}$$

where

$$\frac{\mathrm{d}\sigma_{\text{prim}}(M_0)}{\mathrm{d}x_F} = \sum_{\{i,j\}} \sigma_{\text{eff}}^{ij}(M_0) \frac{\mathrm{d}I_{ij}(\tau_0)}{\mathrm{d}x_F} \tag{III.8}$$

with

$$\frac{\mathrm{d}I_{ij}(\tau_0)}{\mathrm{d}x_F} = \frac{\tau_0}{\sqrt{x_F^2 + 4\tau_0}} f_i(x_1) f_j\left(\frac{\tau_0}{x_1}\right), \tag{III.9}$$

x_1 being equal to $\frac{1}{2}(x_F + \sqrt{x_F^2 + \tau_0})$. The quantity $(\mathrm{d}N/\mathrm{d}x_F)(x_F')$ is the distribution of the x_F variable for the meson M_0 issued from the (isotropic) decay of meson M_1 ($M_1 \to M_0 + M_2$, M_2 possibly effective) with x_F':

$$\frac{\mathrm{d}N}{\mathrm{d}x_F}(x_F') = \frac{M_1^2}{\sqrt{(M_1^2 - \Sigma^2)\,(M_1^2 - \Delta^2)}\sqrt{x_F'^2 + 4\tau_1}} \tag{III.10}$$

with

$$\Sigma = M_0 + M_2, \quad \Delta = M_0 - M_2. \tag{III.11}$$

Finally, the integration boundaries in (III.7) are given by

$$\begin{Bmatrix} x'_{F,\mathrm{up}} \\ x'_{F,\mathrm{low}} \end{Bmatrix} = \pm \frac{\sqrt{(M_1^2 - \Sigma^2)\,(M_1^2 - \Delta^2)}}{2M_0^2} \sqrt{x_F^2 + 4\tau_0} + \frac{M_1^2 + M_0^2 - M_2^2}{2M_0^2} x_F. \quad \text{(III.12)}$$

If one neglects the mass differences between parent M_1 and daughter M_0 (same hypothesis as to pass from (III.5) to (III.6)), we can approximate (III.7) by

$$\frac{\mathrm{d}\sigma^{\mathrm{tot}}(M_0)}{\mathrm{d}x_F} \approx \sum_{\{i,j\}} \sigma_{\mathrm{eff}}^{ij,\mathrm{tot}}(M_0) \frac{\mathrm{d}I_{ij}(\tau_0)}{\mathrm{d}x_F}, \quad \text{(III.13)}$$

with the $\sigma_{\mathrm{eff}}^{ij,\mathrm{tot}}(M_0)$ defined at (III.6). This relation has basically the same structure as formula (3.4) for the total cross-section[1].

To compare differential cross-sections at different $\sqrt{s}$, one often prefers to use the rapidity variable y

$$y = \frac{1}{2} \ln \left(\frac{\sqrt{x_F^2 + 4\tau_0} + x_F}{\sqrt{x_F^2 + 4\tau_0} - x_F} \right), \quad x_F = 2\sqrt{\tau_0} \sinh(y). \quad \text{(III.14)}$$

One easily obtains differential cross-sections versus y from above:

$$\frac{\mathrm{d}\sigma}{\mathrm{d}y} = \sqrt{x_F^2 + 4\tau_0} \left. \frac{\mathrm{d}\sigma}{\mathrm{d}x_F} \right|_{x_F = x_F(y)} = 2\sqrt{\tau_0} \cosh y \left. \frac{\mathrm{d}\sigma}{\mathrm{d}x_F} \right|_{x_F = x_F(y)}. \quad \text{(III.15)}$$

Recalling (III.8) and (III.13), one obtains

$$\frac{\mathrm{d}\sigma_{\mathrm{prim}}(M_1)}{\mathrm{d}y} = \sum_{\{i,j\}} \sigma_{\mathrm{eff}}^{ij}(M_1) \frac{\mathrm{d}I_{ij}(\tau_1)}{\mathrm{d}y} \quad \text{(III.16)}$$

and another equation for the differential cross-section, which, in the same approximation as (III.13), writes

$$\frac{\mathrm{d}\sigma^{\mathrm{tot}}(M_0)}{\mathrm{d}y} \approx \sum_{\{i,j\}} \sigma_{\mathrm{eff}}^{ij,\mathrm{tot}}(M_0) \frac{\mathrm{d}I_{ij}(\tau_0)}{\mathrm{d}y} \quad \text{(III.17)}$$

with

$$\frac{\mathrm{d}I_{ij}(\tau_0)}{\mathrm{d}y} = \tau_0 f_i(x_0) f_j\left(\frac{\tau_0}{x_0}\right) \quad \text{(III.18)}$$

and

$$x_0 = \sqrt{\tau_0} e^y. \quad \text{(III.19)}$$

IV. Analysis of J/ψ production

A. Introduction

Our goal is to determine the quantities $\sigma_{\mathrm{eff}}^{ij,\mathrm{tot}}$ [entering (III.4) and (III.17)] for J/ψ production, the quantities σ_{prim} (III.2) for J/ψ, χ and ψ' and $\sigma_{\mathrm{eff}}^{ij}$ for J/ψ production (at some c.m. energy at least). The method amounts to calculate the quantities I^{ij} and to compare the expressions to the experimental data, trying to fit the whole body of existing data. One may wonder whether this procedure is valid, since the structure functions are known to some accuracy only. However, the structure functions are rather well-known for $x \gtrsim 0.1$, and we will see that the bulk of data are not sensitive upon the various parametrizations in this range of values of x. We will illustrate this point below. In the following, we use the Morfin and Tung (fit B1) [7] parametrization of the structure functions, unless explicitly stated.

It is sometimes stated that the J/ψ production data could be used to get information about the structure functions. It is true that these data could provide information on the gluon structure function at small x. This does not introduce any methodological problem in our analysis, since the structure functions of [7] have been determined from lepton-nucleon deep inelastic scattering and Drell–Yan processes, and not from J/ψ production.

B. J/ψ production

We first concentrate on inclusive J/ψ production. To simplify our notation we rewrite $\sigma_{\mathrm{eff}}^{ij,\mathrm{tot}}$ as $\sigma^{q\bar{q}}$ or σ^{gg}. As an example, (III.4) becomes

$$\sigma^{\mathrm{tot}}(J/\psi) = \sigma^{gg} I_{gg}(\tau_{J/\psi}) + \sigma^{q\bar{q}} I_{q\bar{q}}(\tau_{J/\psi}). \quad \text{(IV.1)}$$

where, in fact,

$$I_{q\bar{q}} = I_{u\bar{u}} + I_{\bar{u}u} + I_{d\bar{d}} + I_{\bar{d}d} + I_{s\bar{s}} + I_{\bar{s}s}. \quad \text{(IV.2)}$$

The experimental data for the $pp \to J/\psi + X$ reaction are given in Fig. 2 along with two fits, corresponding to either pure gg or pure $q\bar{q}$ processes. Although the $q\bar{q}$ fit is a little bit better, these data alone are not good enough to constrain the fit in such a way to allow a determination of σ^{gg} and $\sigma^{q\bar{q}}$. In Fig. 3 we present the existing data on the $p\bar{p} \to J/\psi + X$ reaction, still along with the fits for either pure gg or $q\bar{q}$ processes. Here, the data are roughly consistent with a pure $q\bar{q}$ process. However, if one takes the lowest energy point seriously, the $p\bar{p} \to J/\psi + X$ data allow for some gg process. When one tries to determine good fits (allowing a mixture of gg and $q\bar{q}$ processes) to the pp and $p\bar{p}$ data simultaneously, one obtains the dotted lines shown in Fig. 4 with the indicated values of σ^{gg} and $\sigma^{q\bar{q}}$. However, the χ^2 function is very flat. The value of σ^{gg} may deviate by ≈ 44 nb from the best value before the χ^2 is multiplied by 2. Similarly, the value of $\sigma^{q\bar{q}}$ may deviate by ≈ 100 nb.

The larger (though limited) sensitivity of the $p\bar{p}$ data in the fitting procedure is explained by the behaviour of the I_{ij} quantities with the τ variable (see Fig. 5). The quantity $I_{q\bar{q}}$ is much flatter in the $\bar{p}p$ or $\bar{p}n$ case than in the pp case. The quantities $I_{q\bar{q}}$ tend to the same values for small τ, i.e. for large s because, in these conditions, the contribution to the $I_{q\bar{q}}$ integrals comes from the small x part of the structure functions which is dominated by the sea quarks and which is approximately the same in protons and antiprotons.

The ratio $\sigma(pp \to J/\psi + X)/\sigma(p\bar{p} \to J/\psi + X)$, if ideally measured, would determine the ratio $\sigma^{gg}/\sigma^{q\bar{q}}$. Unfortunately, as shown in Fig. 6, the data are not of good

[1] in the analysis below, we, of course, use expressions (III.7–III.8)

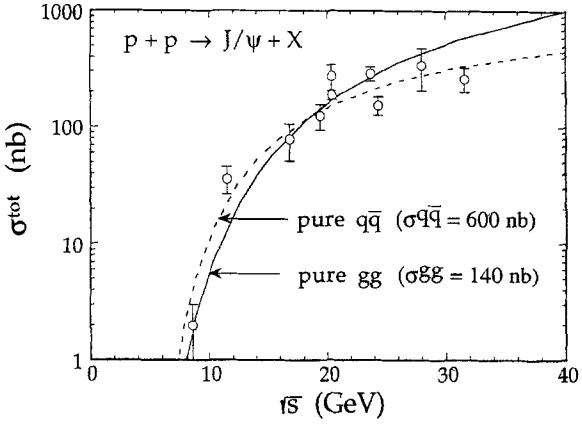

Fig. 2. Comparison of the experimental data [8, 9, 16–24] for J/ψ production as a function of the pp c.m. energy with (III.4) assuming either a pure gg or a pure $q\bar{q}$ contribution, with in each case the best value of the effective total cross-sections $\sigma_{\text{eff}}^{ij,\text{tot}}$

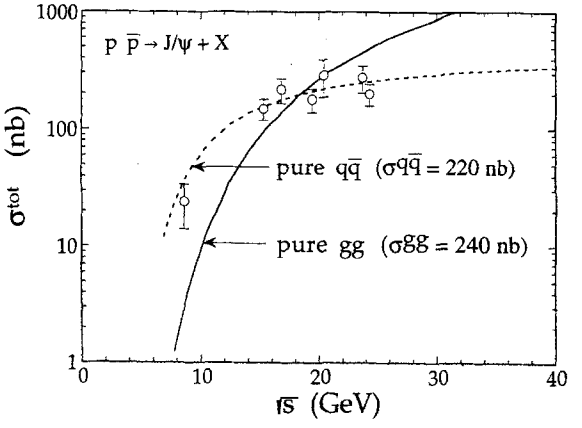

Fig 3. Same as Fig. 2 for J/ψ production in $p\bar{p}$ collisions. The experimental data are from [9, 17, 20–22, 25]

quality and are barely consisting with values of $\sigma^{gg}/\sigma^{q\bar{q}}$ between ~ 0.3 and 3. Figure 3 also corroborates that the best fit of the integrated cross-sections is consistent with $\sigma^{gg} \approx \sigma^{q\bar{q}}$, with large uncertainty. It is nevertheless interesting to note that no data point lies under the $\sigma^{gg} = 0$ curve.

C. Differential cross-section at $y = 0$

We use the formulae of Sect. III expressing $\left.\frac{d\sigma^{\text{tot}}}{dy}\right|_{y=0}$ in terms of σ^{gg} and $\sigma^{q\bar{q}}$ (see (III.15)–(III.19)). The excitation function for the differential cross-section for $pp \to J/\psi + X$ at $y = 0$ is given in Fig. 7 with fits assuming pure gg or pure $q\bar{q}$ processes. The data definitely require a mixing of both contributions, with a large $q\bar{q}$ contribution. Indeed, we performed a simultaneous fit of the inclusive total production cross-section in pp and $p\bar{p}$ and of the differential pp cross-section at $y = 0$. The best fit is obtained for $\sigma^{gg} = (25 \pm 1.5)$ nb and $\sigma^{q\bar{q}} = (232 \pm 19)$ nb and corresponds to the full curves in Fig. 4 and in the bottom of Fig. 7. The indicated errors are purely

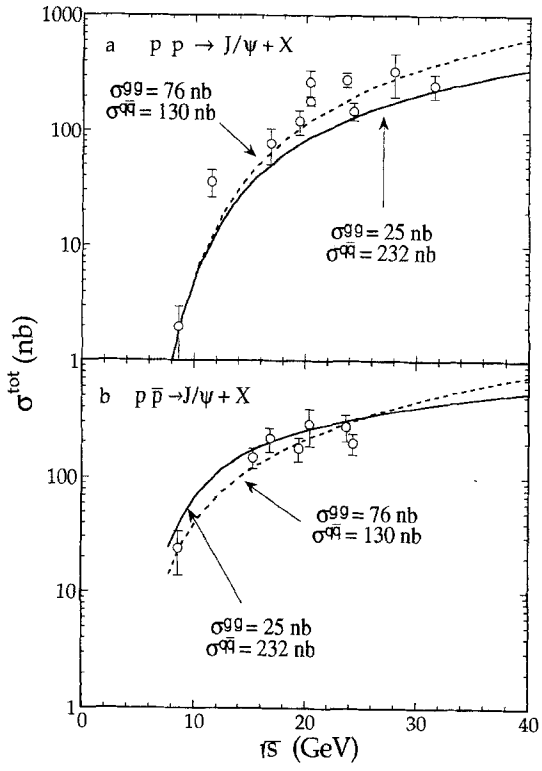

Fig. 4. a Comparison of the experimental J/ψ production cross-sections in pp collisions with (III.4) using the indicated values of the effective total cross-sections. **b** Same for J/ψ production in $p\bar{p}$ collisions

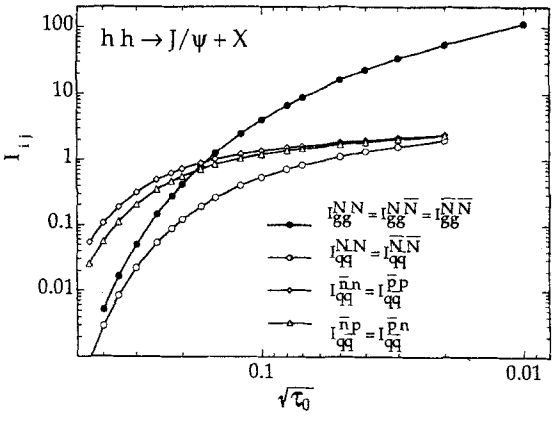

Fig. 5. Numerical values of $I_{ij}^{h_1 h_2}(\tau_0)$ [see (III.1) and (III.2)]relative to J/ψ production in various systems. Notice the unusual scale for the abscissa

statistical, assuming the error bars on the data of purely statistical origin and the χ^2 being a real χ^2 stochastic variable. The dispersion of the experimental data clearly points to the presence of systematic errors. The latter may be tentatively determined by looking at the variation of the fitted parameters necessary to double to optimum χ^2 value (which is 6.35 in this case). One would then obtain $\sigma^{gg} = (25 \pm 15)$ nb and $\sigma^{q\bar{q}} = (232 \pm 55)$ nb.

It is worthwhile to mention that the errors brought by the uncertainty of the structure functions are much

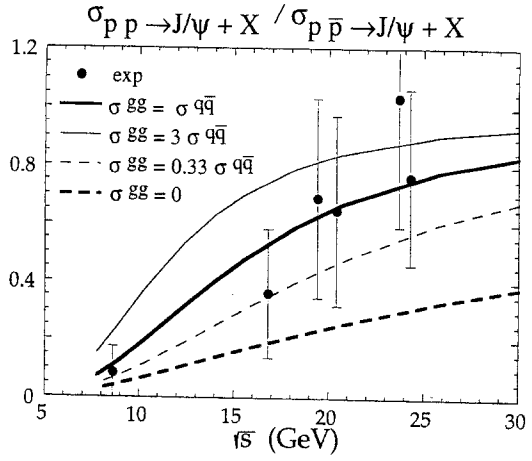

Fig. 6. Ratio between the J/ψ production cross-sections in pp and $p\bar{p}$. Comparison between experimental values and formula (III.4) for various ratios of the effective total cross-sections

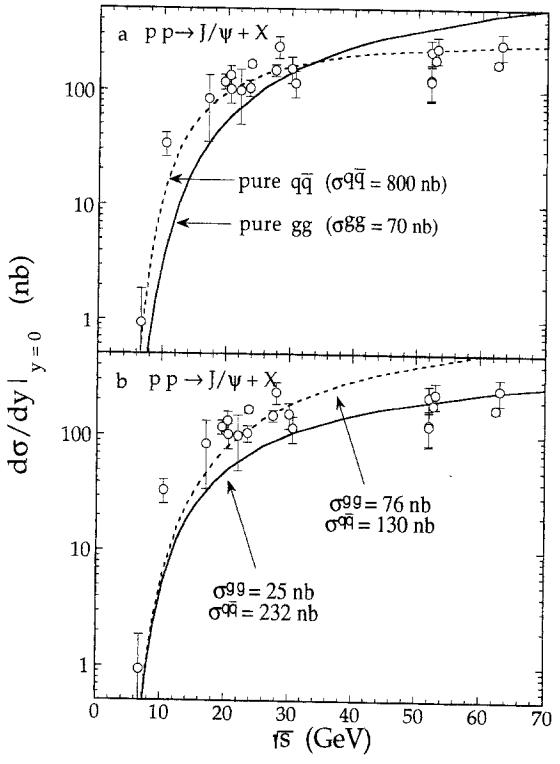

Fig. 7. a Comparison between experimental values of the differential J/ψ cross-section at $y = 0$ with formula (III.17), assuming the indicated effective total cross-sections. The data are taken from [8, 9, 16, 18, 26–29]. **b** Fits with different values of the total effective cross-sections

smaller than the systematic errors. The best fit obtained with the structure functions of [10] yield $\sigma^{gg} = (30 \pm 1.9)$ nb and $\sigma^{q\bar{q}} = (227 \pm 19)$ nb, with statistical errors, i.e. very close to the values indicated above.

It should be mentioned that the $y = 0$ differential cross-section constrains the fit to large values of $\sigma^{q\bar{q}}$, mainly because of the higher energy ($\sqrt{s} \approx 50$ GeV) points (see Fig. 7).

Summarizing the analysis up to now, the cross-sections for J/ψ production in pp and $p\bar{p}$, integrated or at $y = 0$, appear to require a mixing of the gg and $q\bar{q}$ processes. The best fit of all data leads to $\sigma^{q\bar{q}} \approx 232$ nb and $\sigma^{gg} \approx 25$ nb. The total gg and $q\bar{q}$ contributions, including the phase space factors, are approximately in the ratio 1:2 at $\sqrt{s} \approx 20$ GeV (where $I_{gg}/I_{q\bar{q}} \approx 4$).

D. Differential cross-section for $pp \to J/\psi + X$

Figure 8 shows the two existing sets of data for $\sqrt{s} = 20.5$ GeV [8] and $\sqrt{s} = 23.7$ GeV [9]. One has unfortunately to underline the inconsistency of the data. One would expect a broader distribution in rapidity for the larger available energy, whereas the data seem to indicate the contrary. Furthermore, integrated cross-sections differ by $\sim 50\%$. One can however look to the x_F distribution to see what kind of constraints it implies. In Fig. 9, we show the data of Branson et al. [8] along

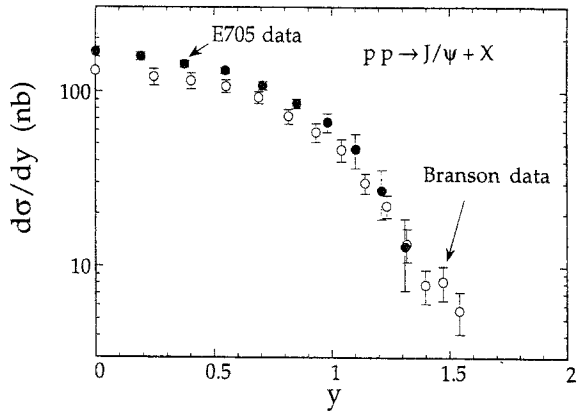

Fig. 8. Experimental data for the differential J/ψ production cross-section versus the rapidity at pp c.m. energy equal to 20.5 GeV (*open dots* [8]) or 23.7 GeV (*black dots* [9])

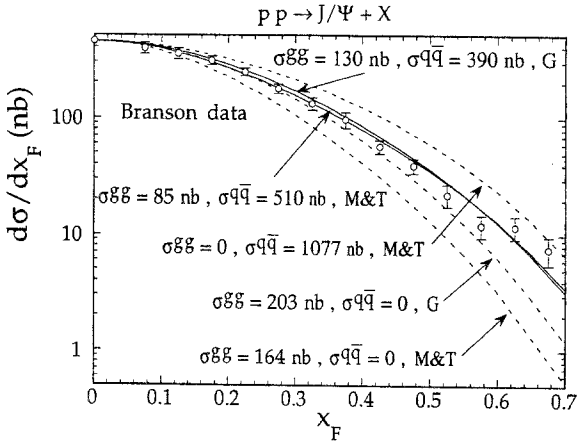

Fig. 9. Comparison of the data of Branson et al. [8] for the differential J/ψ production as a function of x_F, with (III.13) using the parametrization of Glück et al. [10] and Morfin and Tung [7] (respectively denoted by G and M&T) for the gluon structure function (for the quarks, they are equivalent). *Dashed lines* correspond to pure processes (either gg or $q\bar{q}$) and *full lines* to best fits, using mixed processes. In all cases, the total effective cross-sections give were determined to reproduce the experimental point at $x_F = 0$

with the predictions of (III.13) (with the notation (IV.1)) assuming pure gg or pure $q\bar{q}$ processes. In both cases, the effective cross-sections σ^{gg} or $\sigma^{q\bar{q}}$ have been chosen to reproduce $d\sigma/dx_F$ at $x_F = 0$, with $\sigma^{q\bar{q}} = 1077$ nb and $\sigma^{gg} = 164$ nb, respectively. In differential cross-sections, the sensitivity to the structure functions parametrization is higher, because large x_F imply values of x at which they are less precisely known (especially the gluon one). For this reason, we have also made the calculation assuming Glück et al. [10] parametrization of the gluon structure function. In this case, $\sigma^{gg} = 203$ nb.

These σ^{gg} and $\sigma^{q\bar{q}}$ values are larger than the values quoted in Sect. IV.B, because the latter are determined by an overall fit of the excitation functions whereas the two points at $\sqrt{s} = 20.5$ and 23.7 GeV are lying above the general trend (see Fig. 2). Therefore, the differential cross-section data should not be used for determining the *absolute* values of σ^{gg} and $\sigma^{q\bar{q}}$, but the x_F dependence may be used to constrain their ratio.

If a pure $q\bar{q}$ contribution is assumed, the differential cross-section is largely overestimated at large x_F. If the parametrization of Morfin and Tung is used, the pure gg contribution is definitely too small at large x_F. Some mixing seems necessary; the σ^{gg} and $\sigma^{q\bar{q}}$ producing the best fit are 85 nb and 510 nb respectively, with a ratio $\sigma^{gg}/\sigma^{q\bar{q}} = 1/6$ consistent with the one obtained in Sects. IV.B and IV.C. If the parametrization of Glück et al. [10] is used, the pure gg contribution also underestimates the data at large x_F. Here, the best fit is given by $\sigma^{gg} = 130$ nb and $\sigma^{q\bar{q}} = 390$ nb, with a ratio $\sigma^{gg}/\sigma^{q\bar{q}} = 1/3$.

It is perhaps not recommended to attach too much weight to the large x_F points in this analysis, as they may be contaminated by the intrinsic charm contribution, if any. Nevertheless, if one restricts to $x_F \lesssim 0.4$, it is clear that the x_F shape of the data requires a mixing of gg and $q\bar{q}$ contributions. In this range of x_F, the Morfin and Tung and Glück et al. parametrizations are equally good. They give a ratio $\sigma^{gg}/\sigma^{q\bar{q}}$ which is consistent with the value obtained by our fit above.

In Fig.10, we present the data of Antoniazzi et al. [9] and the theoretical curves, assuming either pure $q\bar{q}$ process, with $q\bar{q} = 1090$ nb, or pure gg process with $\sigma^{gg} = 139$ nb (179 nb) using the Morfin and Tung (Glück et al.) parametrization of the structure functions. The conclusions are qualitatively the same as for the Branson data [8], with however a larger importance of the gg process.

In conclusion, the large x_F data seem to favour the Morfin and Tung parametrization. However, better (and consistent) data and a better understanding of the intrinsic charm effects are needed before drawing definite conclusions. The data at small and moderate x_F are consistent with the $\sigma^{gg}/\sigma^{q\bar{q}}$ ratio indicated by our best fit.

E. ψ' production

The existing experimental data for the $\psi'/(J/\psi)$ ratio for the total cross-section or the differential cross-section at $y = 0$ are given in Fig. 11 (for the $p\bar{p}$ case, this figure is only an indication, since the data are very poor). Roughly speaking, this ratio is approximately equal to 0.1. Figure

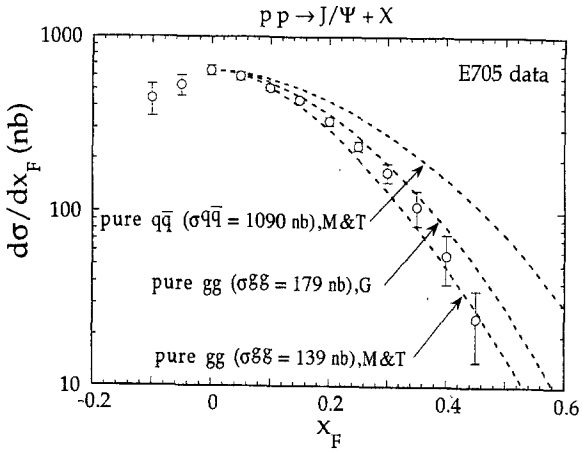

Fig. 10. Same as Fig. 9 for the experimental data of [9], using the indicated effective cross-sections and structure function parametrizations

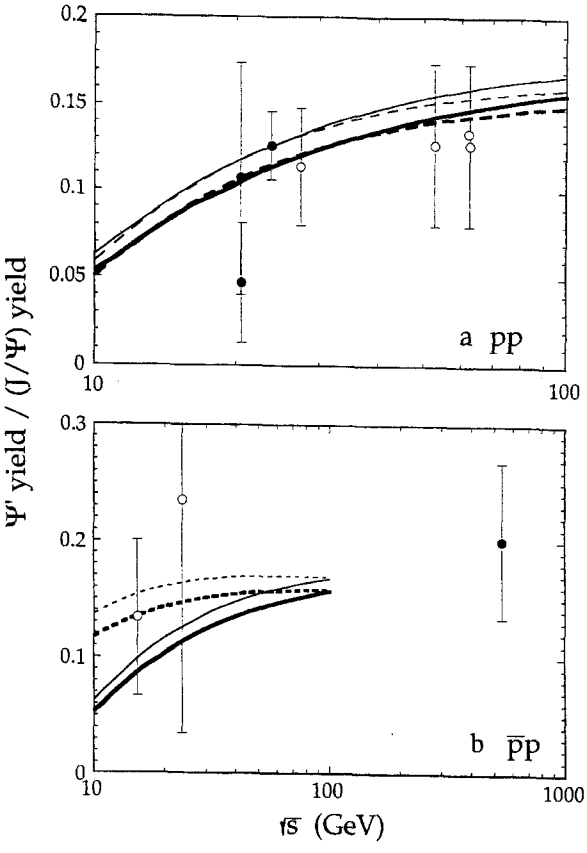

Fig. 11. **a** Experimental data for the ratio $\psi'/J/\psi$ in pp collisions. The *open dots* refer to the differential cross-section at $y = 0$ and the *black dots* to the total cross-sections. The data are from [8, 9, 18, 25]. Full and *dashed thin lines* correspond to the ratio of $y = 0$ differential cross-sections (issued from (III.16) for ψ' and (III.17) for J/ψ), for pure gg and $q\bar{q}$ processes respectively. *Full* and *dashed thick lines* correspond to the ratio of total cross-sections (issued from (III.2)-for ψ'-over (III.4)- for J/ψ-), for pure gg and $q\bar{q}$ processes respectively. Ratios $\sigma^{gg}_{\text{eff}}(\psi')/\sigma^{gg,\text{tot}}_{\text{eff}}(J/\psi) = 1/5$ (for pure gg processes) or $\sigma^{q\bar{q}}_{\text{eff}}(\psi')/\sigma^{q\bar{q},\text{tot}}_{\text{eff}}(J/\psi) = 1/6$ (for pure $q\bar{q}$ processes) are used. **b** Same as in (**a**) for the $p\bar{p}$ collisions. Data are from [8, 25, 31]. Same values as above have been taken for the ratios $\sigma^{gg}_{\text{eff}}(\psi')/\sigma^{gg,\text{tot}}_{\text{eff}}(J/\psi)$ and $\sigma^{q\bar{q}}_{\text{eff}}(\psi')/\sigma^{q\bar{q},\text{tot}}_{\text{eff}}(J/\psi)$

11 also shows that the (smooth) variation of this ratio parallels the one of $I_{gg}(\psi')/I_{gg}(J/\psi)$, $(dI_{gg}(\psi')/dy|_{y=0})/(dI_{gg}(J/\psi)/dy|_{y=0})$, $I_{q\bar{q}}(\psi')/I_{q\bar{q}}(J/\psi)$ and $(dI_{q\bar{q}}(\psi')/dy|_{y=0})/(dI_{q\bar{q}}(J/\psi)/dy|_{y=0})$. This suggests that, within the (large) experimental uncertainty, the effective cross-section for the ψ' production and the effective total cross-sections for the J/ψ final production are roughly in the same ratio. Assuming pure gg process, the ratio $\sigma^{gg}(\psi')/\sigma^{gg}(J/\psi)$ should be of the order of 1/5. Assuming pure $q\bar{q}$ process, one gets similar results with a ratio $\sigma^{q\bar{q}}(\psi')/\sigma^{q\bar{q}}(J/\psi)$ of the order of 1/6. Note that only one effective cross-section ratio is needed to reproduce at the same time total *and* differential results for the *pp and* $p\bar{p}$ reactions; this consistency reinforces the confidence we have in the effective cross-section picture.

Also for the pure $q\bar{q}$ process, note from Fig. 11b the higher $\psi'/(J/\psi)$ ratio in $p\bar{p}$ reaction compared to pp reaction, due to a flatter behaviour of $I_{q\bar{q}}^{p\bar{p}}$ compared to $I_{q\bar{q}}^{pp}$ (see Fig. 5) and so, a value of $I_{q\bar{q}}^{p\bar{p}}(\psi')/I_{q\bar{q}}^{p\bar{p}}(J/\psi)$ higher than $I_{q\bar{q}}^{pp}(\psi')/I_{q\bar{q}}^{pp}(J/\psi)$ (the same explanation holds for the differential production at $y=0$). We see here a way to possibly disentangle $q\bar{q}$ from gg processes in ψ' production, as soon as better data are available.

F. J/ψ production via the χ's

In some cases, this production cross-section has been measured by the detection of a γ (within the required energy range) in coincidence with the dilepton resulting from the decay of the J/ψ. Figure 12 gives the existing data and underscores crually the lack of good quality data.

If one assumes that the χ is produced by gg contribution only (which is an assumption stronger than the ones which constitute our general framework), one may write

$$\frac{\sigma(\chi \to J/\psi + \gamma)}{\sigma^{\text{tot}}(J/\psi)} = \frac{\sigma^{gg}(\chi) I_{gg}(\tau_\chi) BR(\chi \to J/\psi + \gamma)}{\sigma^{gg}(J/\psi) I_{gg}(\tau_{J/\psi}) + \sigma^{q\bar{q}}(J/\psi) I_{q\bar{q}}(\tau_{J/\psi})}. \tag{IV.3}$$

In the energy range considered in Fig. 12, this ratio is about 0.3. The branching ratio (averaged for χ_1 and χ_2)

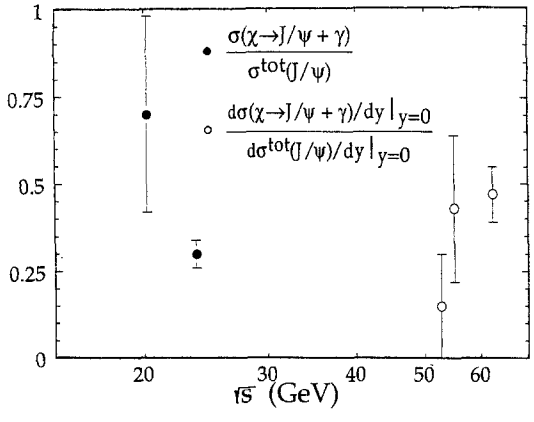

Fig. 12. Experimental data for the fraction of J/ψ production coming from the χ. The *open dots* refer to the differential cross-section at $y=0$ and the *black dots* to the integrated cross-section. Data are from [12, 29, 32, 33]

≈ 0.2. Using the previously determined value of $\sigma^{gg}(J/\psi)$ and $q\bar{q}(J/\psi)$, one finds roughly $\sigma^{gg}(\chi) \approx 173$ nb around $\sqrt{s} \approx 20$ GeV. (This in fact can be viewed as a lower limit). In the frame of the same hypothesis (adopted in the two gluon fusion model), the $\chi \to J/\psi + \gamma$ contribution to the effective cross-section σ^{gg} for J/ψ production is given [see (III.5)] by

$$\sigma^{gg}(\chi \to J/\psi + \gamma) = \sigma^{gg}(\chi) BR(\chi \to J/\psi + \gamma) \times I_{gg}(\tau_\chi)/I_{gg}(\tau_{J/\psi}). \tag{IV.4}$$

Numerically, for $\sqrt{s} \approx 20$ GeV, this cross-section amounts to ≈ 24 nb, close to our best fit value.

G. Summary

In conclusion, adopting as few assumptions as possible, we have determined from the excitation functions of total pp and $\bar{p}p$ cross-sections and of the $y=0$ pp differential cross-section, that the best values of the effective total cross-sections for the $q\bar{q}$ and gg processes are

$$\sigma^{q\bar{q}}(J/\psi) \approx (232 \pm 55) \text{ nb}, \quad \sigma^{gg}(J/\psi) \approx (25 \pm 15) \text{ nb}, \tag{IV.5}$$

with statistical and systematic errors. The rest of the data helped us to give independent error bars on the ratio $\sigma^{gg}/\sigma^{q\bar{q}}$. Unfortunately, the low quality of the data is such that we were only able to determine that this ratio lies between 1 and 1/10, i.e. consistent with the result (IV.5). We stress that this conclusion has been reached by the simultaneous analysis of all data and without recourse of any detailed dynamical model. As a consequence, the effective cross-sections include all the successive steps of meson production, including colour neutralisation and final decays. In the next section, we will attempt to extract the primordial cross-sections at one energy.

Our analysis points to a large $q\bar{q}$ contribution, partly because they include the $y=0$ pp data at $\sqrt{s} \gtrsim 50$ GeV. If these points had to be ignored (they are rather old data), the $\sigma^{q\bar{q}}$ value would nevertheless still be twice as large as the σ^{gg} value. In other words, the $q\bar{q}$ contribution seems to be larger than what it is sometimes suggested. In particular, this seems to disagree to recent $\mathcal{O}(\alpha_s^3)$ QCD calculations [34–36]. Reference [36] predicts $\sigma^{gg} \approx 160$ nb and $\sigma^{q\bar{q}} \approx 4$ nb. However, one has to underline that this refers to $\sqrt{s} = 100$ GeV, substantially larger than the typical energies $\sqrt{s} = 10$–30 GeV, that we were looking at.

The poor quality of the experimental data does not allow to be very precise in the conclusion. The extraction of the (mainly gluon) structure functions cannot be performed in such a situation. However, we have seen that integrated or small x_F cross-sections are not very sensitive to the structure functions (in the range where they are badly known). Therefore, the strategy is well defined. As soon as good data are obtained on integrated or small x_F cross-sections, one will be able to determine the $\sigma^{q\bar{q}}$ and σ^{gg} accurately and ultimately, the structure functions could be determined by the analysis of good large x_F data, provided the contribution of intrinsic charm is clarified.

V. Primodial production of charmonium states

From (III.3) and particularizing to the charmonium states, one may write using (average values of) branching ratios given by[11]

$$\sigma^{\text{tot}}(J/\psi) = \sigma_{\text{prim}}(J/\psi) + 0.273\sigma_{\text{prim}}(\chi_1) + 0.135\sigma_{\text{prim}}(\chi_2) + (0.57 + 0.08\times 0.273 + 0.08\times 0.135)\sigma_{\text{prim}}(\psi') \tag{V.1}$$

or

$$\sigma^{\text{tot}}(J/\psi) = \sigma_{\text{prim}}(J/\psi) + 0.273\sigma_{\text{prim}}(\chi_1) + 0.315\sigma_{\text{prim}}(\chi_2) + 0.6\,\sigma_{\text{prim}}(\psi') \tag{V.2}$$

and

$$\sigma^{\text{tot}}(\psi') = 0.4\,\sigma_{\text{prim}}(\psi'). \tag{V.3}$$

The last two terms of the parenthesis in (V.1) account for the decay $\psi' \to (\chi_1, \chi_2) \to J/\psi$. We have neglected the unknown possible feeding from heavier charmonium states. That is presumably justified by their large widths for $D\bar{D}$ decay. The cross-sections (V.2) and (V.3) are the cross-sections which would be obtained by measuring the abundances by *all* the decays of J/ψ and ψ' except for the ones which are explicitly indicated. What is actually measured is the cross-section for some dilepton decays.The measured cross-sections are then related to the above ones by

$$\sigma_{\text{dil}}(J/\psi) = BR(J/\psi \to l\bar{l})\,\sigma^{\text{tot}}(J/\psi) \tag{V.4}$$

and

$$\sigma_{\text{dil}}(\psi') = BR(\psi' \to l\bar{l})\,\sigma_{\text{prim}}(\psi'). \tag{V.5}$$

The cross-section for the $\chi \to J/\psi + \gamma$ decay is given by

$$\sigma_{\text{dil},\gamma}(\chi \to J/\psi\gamma) = BR(J/\psi \to l\bar{l})\sigma(\chi \to J/\psi\gamma) \tag{V.6}$$

with

$$\sigma\,(\chi \to J/\psi\gamma) = [0.273\,\sigma_{\text{prim}}(\chi_1) + 0.135\,\sigma_{\text{prim}}(\chi_2)] + 0.03\,\sigma_{\text{prim}}(\psi'). \tag{V.7}$$

For later purpose, we rewrite (V.2) as

$$\sigma^{\text{tot}}(J/\psi) = \sigma_{\text{prim}}(J/\psi) + \sigma(\chi \to J/\psi\gamma) + \sigma(\psi' \to J/\psi) \tag{V.8}$$

with

$$\sigma(\psi' \to J/\psi) = 0.57\,\sigma_{\text{prim}}(\psi'). \tag{V.9}$$

There are only two energies where the three quantities (V.4)–(V.6) have been measured, and only one with a good accuracy, namely [11]. At this energy ($\sqrt{s} = 23.7$ GeV), one has,

$$\frac{\sigma_{\text{prim}}(\psi')}{\sigma^{\text{tot}}(J/\psi)} = 0.14 \pm 0.04,$$

$$\frac{\sigma(\chi \to J/\psi\gamma)}{\sigma^{\text{tot}}(J/\psi)} = 0.30 \pm 0.04. \tag{V.10}$$

With these numbers (we quote average values only), we obtain with the help of (V.8) and (V.2)

$$\sigma_{\text{prim}}(J/\psi) = 0.617\ \sigma^{\text{tot}}(J/\psi),$$

$$\sigma_{\text{prim}}(\psi') = 0.140\ \sigma^{\text{tot}}(J/\psi),$$

$$0.273\sigma_{\text{prim}}(\chi_1) + 0.135\ \sigma_{\text{prim}}(\chi_2) = 0.296\ \sigma^{\text{tot}}(J/\psi). \tag{V.11}$$

If, like in the two gluon fusion model, one assumes $\sigma_{\text{prim}}(\chi_1) = 0$, one then obtains $\sigma_{\text{prim}}(\chi_2) = 2.19\sigma^{\text{tot}}(J/\psi)$. If, alternatively, one assumes that $\sigma_{\text{prim}}(\chi_1) = \sigma_{\text{prim}}(\chi_2)$, one obtains $\sigma_{\text{prim}}(\chi_1) = \sigma_{\text{prim}}(\chi_2) = 0.74\ \sigma^{\text{tot}}(J/\psi)$. One can also extract

$$\sigma(\chi \to J/\psi\gamma) = 0.30\sigma^{\text{tot}}\ (J/\psi),$$

$$\sigma(\psi' \to J/\psi) = 0.08\ \sigma^{\text{tot}}(J/\psi). \tag{V.12}$$

These results agree with the number of [12], which carried essentially the same analysis.

Having a measurement at only one energy at our disposal, we cannot extract the quantities σ^{ij}_{eff} of (III.2) from the σ_{prim} without further assumptions. For the sake of illustration, if we assume that the primordial J/ψ production proceeds through $q\bar{q}$ only (which might be consistent with (V.11) and our analysis of Sect. IV), we may write

$$\sigma_{\text{prim}}(J/\psi) = \sigma^{q\bar{q}}_{\text{eff}}(J/\psi) I_{q\bar{q}}(\tau_{J/\psi}). \tag{V.13}$$

At $\sqrt{s} = 23.7$ GeV, $I_{q\bar{q}}(\tau_{J/\psi}) = 0.343$, and we find

$$\sigma^{q\bar{q}}_{\text{eff}}(J/\psi) = 2.92\ \sigma_{\text{prim}}(J/\psi) = 1.8\sigma^{\text{tot}}(J/\psi). \tag{V.14}$$

Assuming the primodial ψ' production proceeding through $q\bar{q}$ also, one finds (with $I_{q\bar{q}}(\tau_{\psi'}) = 0.239$)

$$\sigma^{q\bar{q}}_{\text{eff}}(\psi') = 0.59\ \sigma^{\text{tot}}(J/\psi). \tag{V.15}$$

If we now assume that the primodial χ formation proceeds through the gg channel only, one finds (with $I_{gg}(\tau_\chi) = 1.32$)

$$\sigma^{gg}_{\text{eff}}(\chi_2) = \frac{1}{0.60 + 1.22r}\sigma^{\text{tot}}(J/\psi) \tag{V.16}$$

and

$$\sigma^{gg}_{\text{eff}}(\chi_1) = \frac{r}{0.60 + 1.22r}\sigma^{\text{tot}}(J/\psi), \tag{V.17}$$

If $r = \sigma_{\text{prim}}(\chi_1)/\sigma_{\text{prim}}(\chi_2) = \sigma^{gg}_{\text{eff}}(\chi_1)/\sigma^{gg}_{\text{eff}}(\chi_2)$. For $r = 0$, $\sigma^{gg}_{\text{eff}}(\chi_2) = 1.66\,\sigma^{\text{tot}}\ (J/\psi)$. With the total J/ψ production quoted in [9], namely $\sigma^{\text{tot}}(J/\psi) = 286 \pm 60$ nb, one obtains (with the assumption quoted above) from (V.14) and (V.15) $\sigma^{q\bar{q}}_{\text{eff}}(J/\psi) \approx 515$ nb, $\sigma^{q\bar{q}}_{\text{eff}}(\psi') \approx 169$ nb, and with no primordial χ_1, $\sigma^{gg}_{\text{eff}}(\chi_2) \approx 475$ nb. However, let us recall that the value quoted in [9] lies a factor 2 above the general trend (see Fig. 4). The effective cross-sections should then be corrected accordingly. If we take for σ^{tot} the "general trend" cross-section, given by (III.5) and our

best values for σ^{gg} and $\sigma^{q\bar{q}}$, i.e. 160 nb at $\sqrt{s} = 23.7$ GeV, one has:

$$\sigma^{q\bar{q}}_{\text{eff}}(J/\psi) \approx 288 \text{ nb}, \quad \sigma^{q\bar{q}}_{\text{eff}}(\psi') \approx 94 \text{ nb}, \tag{V.18}$$

and with no primordial χ_1,

$$\sigma^{gg}_{\text{eff}}(\chi_2) \approx 266 \text{ nb}. \tag{V.19}$$

One may check whether these numerical values and the assumptions which enable us to determine the effective cross-sections (V.18)–(V.19) are reasonable. Indeed, we can reconstruct the quantities $\sigma^{q\bar{q}}(J/\psi)$ and $\sigma^{gg}(J/\psi)$ by using (III.5). One has in this case:

$$\sigma^{q\bar{q}}(J/\psi) = \sigma^{q\bar{q}}_{\text{eff}}(J/\psi) + 0.6\sigma^{q\bar{q}}_{\text{eff}}(\psi')\frac{I_{q\bar{q}}(\tau_{\psi'})}{I_{q\bar{q}}(\tau_{J/\psi})} \approx \sigma^{\text{tot}}(J/\psi) \tag{V.20}$$

and

$$\sigma^{gg}(J/\psi) = (0.273\ \sigma^{gg}_{\text{eff}}(\chi_1) + 0.135\sigma^{gg}_{\text{eff}}(\chi_2))\frac{I_{gg}(\tau_\chi)}{I_{gg}(\tau_{J/\psi})}$$
$$\approx 0.15\ \sigma^{\text{tot}}(J/\psi). \tag{V.21}$$

Using the numerical values (V.18) and (V.19), we get

$$\sigma^{q\bar{q}}(J/\psi) \approx 328 \text{ nb}, \quad \sigma^{gg}(J/\psi) \approx 24 \text{ nb}. \tag{V.22}$$

It is reassuring to see that the ratio $\sigma^{gg}(J/\psi)/\sigma^{q\bar{q}}(J/\psi)$ obtained from the multi-resonances production analysis are at *one* energy (namely $\approx 1/13$) at $\sqrt{s} \approx 23.7$ GeV) is not far from the value obtained in Sects. IV.B and IV.C, from the J/ψ production analysis over a wide range in energy (namely $\approx 1/6$). However, the observed resaonable discrepancy probably indicates that the *primordial* production of all the resonances also proceeds through both gg and $q\bar{q}$ channels. The combination of the analysis of Sect. IV and the one of Sect. V at various energies would determine the values of σ^{ij}_{eff} for any pair $\{i,j\}$ and provide at the same time a consistency check of the parton model, as embodied by the equations of Sect. III.

VI. Discussion

In this work, we have tried to separate the gg and the $q\bar{q}$ contributions in charmonium production by pp and $p\bar{p}$ reactions in a manner which is as less model-dependent as possible.Of course, a minimum number of assumptions were necessary. Let us recall them: (1) interaction of two initial partons only; (2) no intrinsic charm effects; (3) colour neutralisation does not affect the energy momentum flow; (4) no internal wave function effects. These assumptions allowed us to write the total cross-section (including decay of unstable resonances) in a closed form which separates the effective cross-sections for the gg and $q\bar{q}$ channels from each other and from the phase space integrals. These features, the different energy variation of the phase space integrals in both channels and for pp and $p\bar{p}$ reactions and the simultaneous fit of the whole body of data permits an extraction of the effective cross-sections.

Before reviewing the results, let us discuss the assumptions above. The first assumption is quite reasonable and generally accepted. In perturbative QCD calculations within the parton model, the interaction of three initial partons appears at one order higher in the perturbation theory. The second assumption is debated in the literature. It is sometimes argued that the intrinsic charm is necessary to explain the A-dependence of the production cross-section on nuclei [13–15], but at a low level anyway. The third assumption is the most critical one and there is no real indication, except in very specific models, of its validity. Our philosophy is to take it as a real assumption and to see whether it allows to describe the data. The removal of the fourth assumption would destroy the factorization between dynamics and phase space. However, this removal is not expected to modify the calculated cross-sections very much, for the J/ψ at least. Therefore, we believe that this assumption does not introduce an uncertainty on our results larger than the one dictated by the accuracy of the data. We insist, however, on the fact that our analysis does not rely on a specific dynamical model (beyond the parton model of the hadrons): lowest order QCD, higher twist, detail of a possible neutralisation process, ...

The total effective cross-sections [quantities entering (III.4)] have been determined to be 232 nb and 25 nb for the $q\bar{q}$ and the gg channels, respectively. The errors are given and discussed in Sect. IV. The importance of the channel contributions themselves, obtained by multiplying by the respective phase space integrals, are approximately in the ratio 2:1 around $\sqrt{s} \approx 20$ GeV. At larger energy, the gg contribution gradually dominates. There are also some indications that the effective cross-sections for the ψ' production and the J/ψ production are roughly in the ratio 1/6.

The measurement of the ψ', the $\chi \to J/\psi$ and the J/ψ production at one energy allows for the reconstruction of the primodial cross-sections and for the evaluation of the $\psi' \to J/\psi$, $\chi \to J/\psi$ contribution to the J/ψ production. For the last case, our result agrees with the analysis of [11]. These kind of measurement made at several energies would allow to disentangle the $q\bar{q}$ and gg importances for the primodial production and would constrain model calculations. As an indication, we have given some numbers for σ^{ij}_{eff}, *assuming* $q\bar{q}$ contribution only to the primodial J/ψ and ψ' production and gg contribution only to χ. In fact, the comparison between the numerical values of $\sigma^{ij,\text{tot}}_{\text{eff}}$, build from values of σ^{ij}_{eff} with relation (III.5) [cf. (V.24)]: $\sigma^{gg,\text{tot}}_{\text{eff}}(J/\psi)/\sigma^{q\bar{q},\text{tot}}_{\text{eff}}(J/\psi) \approx 1/13$) with those extracted at (IV.5) $\sigma^{gg,\text{tot}}_{\text{eff}}(J/\psi)/\sigma^{q\bar{q},\text{tot}}_{\text{eff}}(J/\psi) \approx 1/9$) indicates that these assumptions are not totally valid, even after removal of the local accident in the measured total cross-section (that we mentioned above), which changes nothing on the ratios. Moreover, let us recall that $\sigma^{q\bar{q},\text{tot}}_{\text{eff}}(J/\psi)$ (named simply $\sigma^{q\bar{q}}$ in Sect. IV) is ≈ 232 nb, whereas the indicated $\sigma^{q\bar{q}}_{\text{eff}}(J/\psi)$ is of the order of 288 nb [cf. (V.18)]. Altogether, this probably means that the primordial J/ψ is not solely made by $q\bar{q}$ and involve gg fusion (with some neutralization process) as well.

As we discussed in Sect. V, the extraction of $\sigma^{q\bar{q}}$ and σ^{gg} are practically independent of the details of the structure functions. The latter could in principle be constrained

by looking at the large x_F dependence (and possibly at low energy). Although the data are not of a good quality, it seems that the parametrization of Morfin and Tung is a little bit more adapted to this large x_F region. An obvious extension of our work would be the analysis of the π-proton data in order to put some constraint on the pion structure functions.

References

1. C.E. Carlson, R. Suaya: Phys. Rev. D **18**, 760 (1978)
2. C.H. Chang: Nucl. Phys. B **172**, 425 (1980)
3. R. Baier, R. Ruckl: Z. Phys. C **19**, 251 (1983)
4. S.H. Kuhn: Phys. Lett. B **89**, 385 (1979)
5. H. Fritzsch: Phys. Lett. B **67**, 271 (1977)
6. M. Glück et al: Phys. Rev. D **17**, 2324 (1978)
7. J.G. Morfin, W.K. Tung: Z. Phys. C **52**, 13 (1991)
8. J.G. Branson, et al.: Phys. Rev. Lett. **38**, 1331 (1977)
9. L. Antoniazzi, et al.: Phys. Rev. D **46**, 4828 (1992)
10. M. Glück, E. Reya, A.Vogt: Z. Phys. C **53**, 127 (1992)
11. Particle Data Group: Phys. Rev. D **45**, S1 (1992)
12. L. Antoniazzi, et al.: Phys. Rev. Lett **70**, 383 (1993)
13. S.J. Brodsky, P. Hoyer, C. Peterson, N. Sakai: Phys. Lett. B **93**, 451 (1980)
14. S.J. Brodsky, P. Hoyer, A.H. Mueller, W.K. Tank: Nucl. Phys. B **369**, 519 (1992)
15. G. Chanfray, S. Fleck: Univ. Lyon Preprint (1993)
16. T.M. Antipov, et al.: Phys.Lett. B **76**, 235 (1978)
17. K.A. Anderson, et al.: Phys. Rev. Lett. **42**, 944 (1979)
18. C. Kourkoumelis, et al.: Phys. Lett. B **91**, 475 (1980)
19. C. Kourkoumelis, et al.: Phys. Lett. B **91**, 481(1980)
20. J. Badier, et al.: Z. Phys. C **20**, 101 (1983)
21. M.J. Corden, et al.: Phys. Lett. B **110**, 415 (1982)
22. C. Morel, et al.: Report CERN-PPE/90–127 (1990)
23. E.J. Siskind, et al.: Phys. Rev. D **21**, 628 (1980)
24. EG72 Collaboration Report Fermilab-Pub-90-127 (1990)
25. S. Kastanevas, et al.: Phys. Rev. Lett. **60**, 2121 (1988)
26. F.W. Büsser et al.: Nucl. Phys. B **113** 189 (1976)
27. E. Amaldi, et al.: Nuovo Cimento Lett. **19** 152 (1977)
28. E. Nagy, et al.: Phys. Lett. B **60**, 96 (1975)
29. A.G. Clark, et al.: Nucl. Phys. B 142, 29 (1978)
30. A. Bramberger, et al.: Nucl. Phys. B **134**, 1 (1978)
31. UA1 Collaboration Report CERN-PPE/90-154 (1990)
32. J.H. Cobb et al.: Phys. Lett B **72**, 273 (1977)
33. C. Kourkoumelis, et al.: Phys. Lett. B **81**, 405 (1979)
34. P. Nason, S. Dawson, R.K. Ellis: Nucl. Phys. B **303**, 607 (1988)
35. P. Nason, S. Dawson, R.K. Ellis: Nucl. Phys. B **327**, 49 (1989)
36. W. Beenakker, W.L. Van Neerwen, R. Meng, G.A. Schuler, J. Smith: Nucl. Phys. B **351**, 507 (1991)